NASA DEVELOP National Program
Arizona – Tempe
Spring 2021

San Diego Urban Development

Utilizing NASA Earth Observations to Identify Drivers of Extreme Urban Heat and Generate a High-Resolution Vulnerability Index for Urban Planning and Climate Resiliency in San Diego, California

DEVELOP Technical Report
Final – April 1st, 2021

John Dialesandro (Project Lead)
Meryl Kruskopf
M. Colin Marvin
Mireille Vargas

Advisors:
Dr. Kenton Ross, NASA Langley Research Center (Science Advisor)
Dr. David Hondula, Arizona State University (Science Advisor)

1. Abstract

Exposure to heat exacerbated by an increase in urbanization as well as increasing global temperatures has become a growing concern for cities and their residents. Excess heat can cause increased heat-related morbidity, mortality, and energy costs. Vulnerability to heat-related illnesses is oftentimes correlated to demographics, socioeconomic status, and pre-existing health conditions. The City of San Diego, California boasts 1.4 million residents and, like many other major cities, has experienced increases in heat-related hospitalizations and mortality. The burden of urban heat is also not equal amongst communities; areas with lower income and communities of color bear a disproportionate burden. In partnership with the City of San Diego, and American Geophysical Union's (AGU) Thriving Earth Exchange, the DEVELOP team used Landsat 8 Operational Land Imager (OLI) and Thermal Infrared Sensor (TIRS), and ECOsystem Spaceborne Thermal Radiometer Experiment on Space Station (ECOSTRESS) imagery to identify areas of highest heat based on land surface temperature from 2015-2020. Our analyses showed that health demographics such as obesity and cardiovascular health were the strongest indicators for heat vulnerability. In addition, various inputs (land use/land cover, tree canopy, and building intensity derived from the City of San Diego data along with albedo from Landsat 8) were used in the Integrated Valuation of Ecosystem Services and Tradeoffs (InVEST) urban cooling model to investigate changes in cooling rates in current and future scenarios for the city. The model results showed that cooling is expected to occur due to a 5% increase in tree canopy. The City of San Diego can use these results to inform the development of the Climate Resilient San Diego plan and prioritize at-risk communities for cooling interventions.

Key Terms
InVEST urban cooling model, Landsat 8 TIRS, ECOSTRESS, ecosystem services, heat mitigation, vulnerability, urban heat island

2. Introduction

2.1 Background Information

Urban Heat is a public health hazard that impacts all cities. Excess urban heat exacerbated by extreme heat events has become the leading cause of weather-related deaths, outpacing both floods and wildfires (Weinberger et al., 2017). Outside of mortality, urban heat can cause heat-related illnesses including heatstroke, exhaustion, and amplified respiratory and cardiovascular issues as well as high energy costs (Wald, 2019). Cities in the United States are expected to see increases in temperatures through the twenty-first century and thus increased heat strain on their populations (Krayenhoff et al., 2018).

The City of San Diego is located on the southern California coast. It is home to 1.4 million people, making it the second-largest city in California and eighth largest in the United States. San Diego features a Mediterranean climate according to the Köppen climate classification and receives just over 10 inches of precipitation a year. While the annual mean temperature is only 63°F (17°C), the city can still be

subject to extreme heat events (EHE) with temperatures exceeding 104°F (40°C), particularly in late summer.

The city's planning department is currently working on a climate adaptation and resiliency plan entitled “Climate Resilient San Diego” (Climate Resilient SD) which describes the measures required to increase local capacity to adapt, recover and thrive amidst a changing climate. These adaptation measures include cooling interventions for vulnerable communities. Vulnerable communities are defined by the City's Climate Equity Index which takes into account 35 indicators (such as persons over 75) to measure equity across the city based on nationwide best practices.

In recent years the city has seen increasing urbanization and thus increasing impervious surfaces which result in greater absorption of incoming solar radiation compared to the surrounding unbuilt landscape. This in turn magnifies San Diego’s urban heat island (UHI) and exacerbates heat stress throughout the city (Guirguis, 2018). Climate records support that urban temperatures are increasing (Taha, 2017). Furthermore, climate projection models indicate that coastal areas, like San Diego, can expect 2-3°C (3.5-5.5°F) increases in temperature by mid-century. This would result in as much as 1-2 million additional people being exposed to extreme heatwaves in San Diego from increasing temperatures as well as population growth (Vahmani et al., 2019). The increasing urban temperatures are concerning as they exacerbate the aforementioned health and energy concerns.

Urban heat has been shown to have economic and racial disparities in San Diego. Dialesandro et al. (2021) showed that the lowest income neighborhoods were found to be 2.5°C warmer compared to the wealthiest in San Diego with Latino neighborhoods being over 2°C warmer than white neighborhoods. While these studies provide critical information on UHI disparities they differ from this project in several ways. They utilized data at the block group and zip code resolution to draw conclusions at the county and metro area, while this project focuses on City of San Diego itself (Figure 1). Other studies have showed that it is important to include analysis utilizing specific sociodemographic and health variables since they reveal social vulnerability at an enhanced level compared to other vulnerability analysis done at broader scales such as the county and census tract level (Cooley, 2012). In addition, these studies used remotely sensed data from Landsat 8 Operational Land Imager (OLI) for mapping heat but they did not analyze nighttime temperature.

Figure 1. Study area of the City of San Diego, California (Basemap created with Sentinel-2 data; June 17th, 2019)

2.2 Project Partners & Objectives

The City of San Diego is developing its Climate Resilient SD plan. They are seeking information related to heat risk and vulnerability to identify priority areas for cooling interventions such as increasing urban tree canopy. This project will use factors such as daytime and nighttime land surface temperature and socioeconomic variables (including age above 65, age above 65 and living alone, cardiovascular disease, asthma, hypertension, access to health insurance, language spoken, poverty) to inform decision-making tools and expand the city's current Climate Equity Index.

The city is seeking high-resolution data of temperature and vulnerability throughout the city to better understand the distribution of heat risk. In addition, the partners want to better understand the impact of increased tree canopy on temperatures throughout the city. This project used the Integrated Valuation of Ecosystem Services and Tradeoffs (InVEST) urban cooling model to generate results that highlight opportunities for prioritization of UHI heat mitigation. Insights from this study will guide climate adaptation and resiliency goals for their Climate Resilient SD plan.

3. Methodology

3.1 Data Acquisition

We acquired remotely-sensed data for the study period (1 May – 30 September, 2015-2020) and study area (City of San Diego) from Landsat 8 OLI using Google Earth Engine (GEE). Daytime land surface temperature (LST) and albedo were both derived from the Landsat 8 OLI imagery. Nighttime LST and evapotranspiration (ET) were acquired using data from the ISS ECOSTRESS and filtered by a time period of 2018-2020 June to September (ECOSTRESS had June 2018 launch) from the NASA Application for Extracting and Exploring Analysis Ready Samples (AppEEARS) (Table A1).

Additional datasets included socioeconomic and sociodemographic data from the 2018 American Community Survey (ACS), health data from the Centers for Disease Control and Prevention (CDC) 500 Cities dataset, city and community boundaries, building outlines, and reference datasets from the San Diego open data portal, a collaboration between San Diego Geographic Information Source (SanGIS) and San Diego Association of Governments (SANDAG).

3.2 Data Processing

3.2.1 Land Surface Temperature (LST)

We calculated Daytime LST from the Landsat 8 Surface Reflectance Tier 1 Product. Daytime LST was derived by first filtering available cloud-free imagery between May 1st and September 30th for the years of 2015-2020. This resulted in 42 available images. The script calculated for each image's normalized difference vegetation index (NDVI) to calculate emissivity (E) (Shen et al., 2016), which was then used with the brightness temperature (BT) to calculate LST (Equation 1).

$$LST = BT / (1 + (0.0000115 * BT / 0.01438) * \log(E)) ¿$$

(*Equation 1)*

3.2.2 UHI Magnitude Identification / Urban Heat Maps

The median LST value from the study period was used to create the urban heat maps. Urban heat islands are defined by the deviation in temperature from geographically similar undeveloped areas free of anthropogenic influences. To understand the magnitude of the UHI, we first identified reference areas that represented our study area but had not been urbanized. These sites included the Torrey Pines State Natural Reserve in Northern San Diego, Mission Trails Regional Park, and the Tijuana River Preserve south of the city proper. The UHI magnitude was calculated by taking the difference between the mean LST of a local area and the mean LST of the reference areas. [i]Then we quantified the temperature disparities throughout the thermal environment in San Diego and provided input rural reference temperature and UHI magnitude for the InVEST model.

3.2.3 InVEST Model input data

The InVEST model took a number of required and optional inputs (Table A2). While the optional inputs were explored, the results were not used in the analysis

and there is still considerable investigation to be done to fully understand and utilize this part of the model. See supplemental InVEST Urban Cooling Model Guide for a more thorough discussion. We acquired the remaining data: building outlines, tree canopy, and land use/land cover from the City of San Diego's Open Data Portal and the Regional Data Warehouse, a partnership between the San Diego Association of Governments (SANDAG) and SanGIS. The InVEST urban cooling model relies heavily on land use land cover (LULC) classification and the associated parameters. The resolution of the LULC input determines the specificity of the associated parameters: shade, green area, albedo, and building intensity.

3.2.4 Evapotranspiration (ET) - InVEST Input

We manually chose the 26 ET rasters with 10% or less cloud coverage from 2018-2020 which were processed in ArcGIS Pro. We created a median raster to summarize evapotranspiration for the full study period by inputting the rasters in the 'Cell Statistics' tool in the Spatial Analyst toolbox and selecting the 'median' function. The output was a single raster where each pixel is the median evapotranspiration value across the full study period. We converted the ET values from W m^{-2} to mm day^{-1} and normalized the values before using them as an input for InVEST. The unit conversion was done using a conversion factor in the Food and Agriculture Organization of the United Nations (FAO) Irrigation and Drainage Paper No. 56, Table 1 (Allen et al. 1998) where 0.408 mm day^{-1} = 1 MJ m^{-2} d^{-1}, shown by Equation 2 below.

$$ET_A\ [\text{mm day}^{-1}] = ET_B\ [\text{W m}^{-2}] * 0.0864\ [\text{MJ day}^{-1}]/[\text{W}] * 0.408\ [\text{mm day}^{-1}]/[\text{MJ day}^{-1}\ \text{m}^{-2}]$$

(Equation 2)

where ET_A and ET_B are the numerical values of the evapotranspiration rate in unit of [mm day^{-1}] and [W m^{-2}] respectively

3.2.5 Albedo

The albedo of a surface is critical for understanding how much incoming energy is either absorbed and transformed into heat or reflected into the atmosphere. Each LULC classification has a unique albedo value between 0 and 1, where 0 is complete absorption and 1 is 100% reflectance (no absorption). We calculated the median albedo with a script from the NASA DEVELOP spring 2020 Philadelphia Health & Air Quality project using Equation 3 from Olmedo et al., 2016. We exported the median albedo raster as a TIFF file and brought it into ArcGIS Pro for processing. The Zonal Statistics as Table tool combined albedo information with the LULC vector layer which generated the input for the biophysical table.

3.2.6 Building Intensity

Building Intensity (BI) is the normalized ratio of the floor area to the land area per land use category. It represents the level of urban development; downtown areas would have a high BI while rural areas would have a BI close to 0. To calculate BI, we acquired building outlines from SanGIS and used the Summarize Within tool in ArcGIS Pro to sum the area of the building outlines per each land use category. We manually assigned an average number of floors to each land use category based on the NASA DEVELOP fall 2020 Sacramento Urban Development Appendix B which

was derived from US average building measurements. The total building outline area per land use was multiplied by the average number of floors per that land use category to get the total floor area then divided by the total area of that land use category to get building intensity. These values were then normalized.

3.2.7 Shade

Shade was also generated for the InVEST urban cooling model biophysical table input. The shade values were generated from a tree canopy feature class provided by the City of San Diego. In ArcGIS Pro, we used the Summarize Within tool to find the sum of the tree canopy per each land use category. Dividing by the total land use area produced a percent tree canopy result that was used as the shade input for the biophysical table.

3.2.8. Heat Risk

Heat risk was assessed at two levels. Both census block group and census tract data came from the American Community Survey with the addition of data from the Center for Disease Control (CDC) 500 cities data project for census tract which provides census-tract level estimates of chronic disease risk factors, and health outcomes. These include asthma, hypertension, cardiovascular heart disease, chronic obstructive pulmonary disease (COPD), obesity, and diabetes. We used this shapefile to extract nighttime LST, and daytime LST per census tract, which we then joined in the attribute table. We applied the same process to social-economic data at the block group level but did not include health indicators, poverty percentage, or lack of health insurance percentage due to lack of availability (Table A3).

3.3 Data Analysis

3.3.1 InVEST Urban Cooling Model

The InVEST urban cooling model generates a heat mitigation index (HMI) based on the cooling capacity (CC)of each cell (as defined by the local environmental properties within the cell) and its proximity to green areas. For daytime, the CC-day is a function of shade, albedo, and evapotranspiration index (ETI) (equation 3). ETI is defined as the ET rate of the cell divided by the maximum ET rate in the study area. Note that all three variables in equation 3 take on values between 0 and 1. For nighttime, the CC-night is a function of building intensity (equation 4) since nighttime temperatures are driven by heat release from buildings and impervious surfaces (Ferreira and Duarte, 2019). A third CC associated with the cell (CC-PG) is generated by InVEST related to proximities to green areas. It has been shown that green areas must be bigger than 2 hectares to have a cooling effect on the air around them (MacDonald et al. 2016; Zardo et al. 2017). CC-PG is the sum of the cooling contributions from all nearby green areas with each contribution depending on the CC of the green area and the distance from the cell. The daytime (nighttime) HMI is equal to the larger of the CC-day (CC-night) and CC-PG. With the above definitions, HMI takes on values between 0 and 1.

$$CC-day=(0.6*shade)+(0.2*albedo)+(0.2*ETI)$$

(Equation 3) Cooling capacity for daytime.

$$CC-night=1-Building\ Intensity$$

(Equation 4) Cooling capacity for nighttime.

The ability to model scenarios is dependent on the determination of the albedo and shade which depends on resolution of the LULC layer. The LULC layer provided by the city had 100 categories but the categories were often based on economic and not biophysical characteristics such as automobile dealerships, service stations, or casinos. While these distinctions help with the ability to model different scenarios such as increasing shade at elementary schools but not high schools this also created problems for defining the physical characteristics of these categories especially for categories that had very small areas such as freeways under construction. For this reason, the median albedo was used instead of mean albedo.

Due to the arid climate, it is only feasible to plant trees in areas where irrigation is accessible. For the city, this means road right of way and public spaces such as parks and schools. In addition, the city partners with non-profits who facilitate and incentivize the process of planting trees in residential areas. To model a 5% increase in tree canopy (from approximately 12% to 17%) the shade values in the biophysical table (Table A11) were increased for road right of way, public spaces, and residential categories. In addition, there were small changes in commercial as well. It's important to note that while increasing shade represents an increase in tree canopy, this does not affect the prevalence or influence of "green spaces". In addition, since nighttime HMI is dependent only on building intensity and no land use change was modeled, nighttime model runs only represent existing conditions.

The daytime 5% tree canopy change output was analyzed by looking at the difference in temperature between the existing conditions model run and the five percent increase model run. The model outputs a temperature raster (Tairnom)which is calculated using the equation 5, where Tairref is the reference temperature and UHIMax is the maximum UHI magnitude in the study area . Since the values for the reference air temperature and the UHIMax stay the same for the existing conditions model run and the five percent increase run, the difference in temperature represents the difference in HMI (Equation 5).

$$Tairnom = Tairref + (1 - HMI) * UHIMax$$

(Equation 5)

3.3.2 Heat Exposure and Vulnerability

With the aforementioned model parameters, we created three indices at both the census tract and census block group level for identifying regions that are more vulnerable to heat: 1) a Heat Risk Index 2) Heat Vulnerability Index and 3) Heat Exposure Index. Our Heat Exposure Index used daytime and nighttime LST values with daytime LST values being given a weight half of that of nighttime LST values since research suggests that nighttime temperatures are better predictors of heat-related health outcomes than daytime temperatures (Hajat et al., 2005; Schwartz et al., 2005; Zhang et al., 2012). We used the following equation (Equation 6) to calculate exposure, where mDLSTi and mNLSTi are the mean daytime and nighttime LST values, respectively, for the census tract. The resulting map (Figure 2B) was then ranked by quintile, and classified as very low, low, medium, high and very high priority areas.

$$Exposure = \frac{mDLST * 0.5 + mNLST}{1.5}$$

(Equation 6)

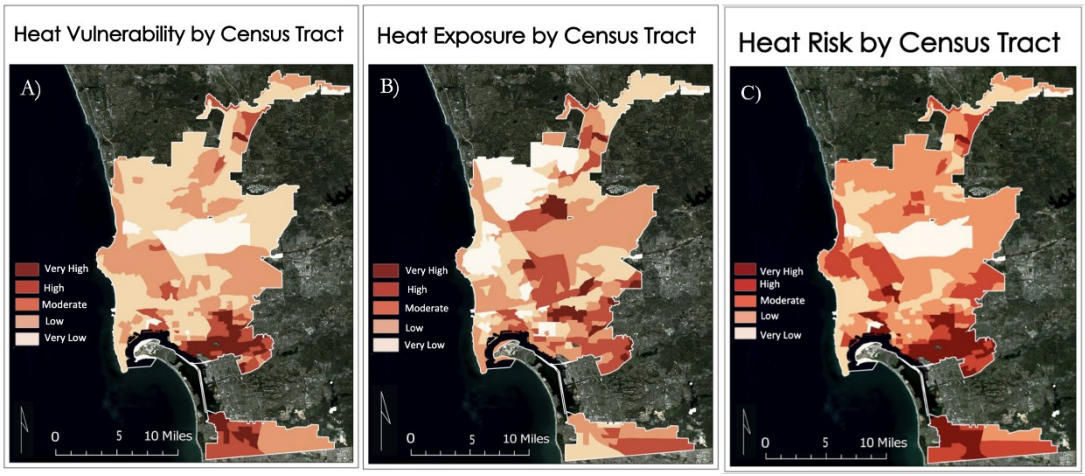

Figure 2: Maps of heat vulnerability (2A), exposure (2B) and risk (2C) at the census tract level for the City of San Diego, California.

The Heat Vulnerability Index is calculated using Principal Component Analysis (PCA). Both social variables and health variables are used at census tract level (Figure 2A). For the census block group (Figure A4), only the social variables are used since health data are not available from CDC at the census group blocks. PCA is a statistical unsupervised method that reduces the dimensionality of a data set by grouping them into linearly uncorrelated principal components that aim to explain most of the data's variance. Because of this, PCA can be used to identify spatial clusters of key factors driving heat vulnerability. Using R, we ran a PCA on our Heat Vulnerability Index by first transforming the input variables to z-scores (mean of 0, standard deviation of 1) to be able to compare the variables which originally had different units and ranges. PCA was done using the principal-function in base R with a varimax rotation. Only principal components that had eigenvalues greater than one were retained (Kaiser, 1960). Components also were required to cumulatively explain approximately 70% of data variance and where the slope is leveling off in the scree plot (Glorfeld, 1995). Based on these criteria and literature, we used four principal components for both the census tract and census block group. Since PCA only detects patterns among input variables, we further evaluated whether the sign, positive or negative, of each component produced by the PCA represented the best current scientific understanding of the real-world relationship between that variable and heat vulnerability-our outcome variable of interest. We then calculated scores for each component and census tract or census block group. Factor scores for each component and census tract were calculated by weighing the z-score of each variable by the 16x4 matrix product of the inverse correlation matrix of the data and the loadings resulting from the PCA. The resulting factor scores were summed to a single score. The same was done at the census block group level but instead using an 8x4 matrix. To visualize heat vulnerability, the overall vulnerability index scores were then ranked

by quintile, and classified as very low, low, medium, high, and very high priority areas (Figure 2A).

Our Heat Risk Index uses normalized values of the Heat Exposure Index and Heat Vulnerability Index and applies Equation 7. We visualized the results of our heat risk index scores by ranking them by quintile, and classifying them as very low, low, medium, high, and very high priority areas for both the census tract (Figure 2C) and census block group (Figure A5) level. These final percentile risk index scores are used to identify areas in San Diego with higher heat risk relative to each other.

$$\textbf{\textit{Risk = Exposure x Vulnerability}}$$

(Equation 7)

4. Results & Discussion

4.1 Analysis of Results

4.1.1 UHI/Hotspot Identification

The City of San Diego is on average 4.1°C (7.3°F) (Figure A8) warmer in the daytime than undisturbed areas or natural landscape patches such as Torrey Pines State Natural Reserve. Throughout the city, temperatures ranged from 20°F cooler in the area's canyons such as Los Penasquitos Canyon near Sorrento Valley and coastal areas near Del Mar and La Jolla to over 30°F near Kearney Mesa and Miramar. Consistently throughout the city the warmest temperatures were areas of high impervious surface, low tree canopy, and barren land such as the case near Miramar and the United States Armed Force Base. The coolest areas were those that had a similar surface complexion as the reference sites (i.e., low amounts of buildings, and roads, tree canopy), as well as areas close to the bay and the Pacific Ocean.

During the nights, the City of San Diego is on average roughly 3°F warmer than areas that were used as reference sites (Figure A9). Throughout the city temperatures ranged from –12°F cooler in areas such as Scripps Ranch community area and Carmel Valley by Los Penasquitos Canyon to 10°F warmer in areas such as Miramar near the military based as well as Mid City: Normal Heights and North Park (Figure A9). While nighttime temperatures have smaller disparities, areas of low tree canopy and higher impervious surface were common traits of nighttime hotspots throughout the city.

4.1.2 Heat Vulnerability- Principal Component Analysis

The PCA run on the census tract level, which included social and health indicators, had 83% of the variance explained with four principal components while the census block group dataset had 84% of the variance explained. The first two principal components for the census tract explained 60% of the variance with the first component explaining 34% of the variance and including all the health indicators (i.e., hypertension, chronic obstructive pulmonary disease, coronary heart disease, asthma, diabetes, and obesity) which all had a strong positive loading (Figure A1). In other words, census tracts that had high populations with hypertension would likely have high populations with chronic obstructive

pulmonary disease and so on. The second principal component included percent of population over 25 years old without a high school diploma, Latinx population, people with no health insurance, limited English proficiency, and percent people below the Federal Poverty Level. The last two principal components, PC3 and PC4, proportionally explained 13% and 10% of the variance respectively.

For the census block group's PCA (Figure A2), the first two principal components explained 54% of the variance in the data. The first principal component contained positive loadings for percent of population over 25 years old without a high school diploma, Latinx population, and limited English proficiency. This reaffirms that there is a strong correlation among these variables since the census block group data did not include health indicators, poverty, or no access to health insurance.

4.1.3 Heat Scores

Heat exposure and social vulnerability had similarities and differences throughout San Diego. Namely, numerous areas had both high exposure and high vulnerability ratings; however, many areas had high exposure and low vulnerability ratings such as areas in the Navajo Community area. For areas of high heat exposure, the communities' areas of Mira Mesa, Mid-City: Normal Heights, College Area, and Skyline-Paradise Hills were the most impacted. The census tract with the highest heat exposure is 06073013103 and its associated census block group, 060730131031, also had the highest exposure (Table A4, Table A8). Areas of lowest exposure were Carmel Valley, Del Mar Mesa, and La Jolla/ University City.

Heat vulnerability at the census tract level (Figure 2 B) was highest in the community areas of Southeastern San Diego, Encanto Neighborhoods, Mid City: Normal Heights, and MidCity Eastern Area. In addition, at the census tract level, we found the southern communities of Otay Mesa-Nestor and San Ysidro to also have high vulnerability. Vulnerability at the block group level reflected that of the census tract analysis except for the Otay Mesa-Nestor and San Ysidro community areas not measuring as highly vulnerable. The census tract with the highest vulnerability is 06073010013 while the census block group with the highest vulnerability is 060730009003 (Table A5, Table A9). Both the census tract's associated census block groups and the census block group's associated census tract were not in the top 10 for heat vulnerability. This discrepancy could be because the analysis of census block groups did not include health, access to healthcare, and poverty indicators.

Our heat risk scores at both the census tract (Figure 2C) and block group (Figure A5) levels showed the communities with the highest heat risk were located in Mid City: City Heights and Eastern Area (Figure A6 and A7). These regions had high populations of people of color, people with no high school education, and people with health problems along with high heat exposure. For example, census block group 060730022012, located in Normal Heights, had a high Latinx population, a high population of people who are isolated and over 65, and a high population with no high school education. Its associated census tract, 06073002201, had a high obesity population and high poverty population. At both the census block group and census tract, there was high daytime and nighttime land surface temperature. The one exception in the agreement between the two levels of analysis was the Rancho Bernard and San Ysidro neighborhoods which were high risk at the census

tract level but not of that at the block group level. This discrepancy can be explained by the lack of poverty, no access to health insurance, and health indicators at the census block group level (Figure A3 and A4). Because of this, our census block group with the highest heat risk did not match up with the census tract with the highest heat risk. At the census block group, the highest score was 060730022011, located in City Heights, which had a high people of color population, a high population of limited English proficiency, and a high population of no high school education. Its associated census tract, 06073002201, had higher than average values for the health, poverty and no access to health insurance indicators (Table A5, Table A6).

4.1.4 InVEST Model Results

The heat mitigation index output for daytime existing conditions generally shows what is expected given our knowledge of the model (Figure 3). Natural areas show up blue and green while more developed areas are shown red-orange to yellow. While open water was classified as a “green area” there is not an extensive cooling effect visible from the coast. This is due to the low values for water for the variables that determine cooling capacity. There is no shade over open water and shade weighted 0.6 so has the biggest influence on CC, albedo is low since water is dark and absorbs energy instead of reflecting it, and ET data is not available over water. The community planning areas of Southeastern San Diego, Mid-City Normal Heights, Encanto, and North Park in the central part of San Diego all had low heat mitigation index values. In the northern portion of San Diego, the Mira Mesa Community planning area also had low heat mitigation index values (Figure 3).

Nighttime HMI (Figure A10) is driven entirely by building intensity. This is apparent as areas with one-story homes in the northern area of the city have a much higher heat mitigation index than areas closer to downtown. Similar to daytime values the community planning areas of Southeastern San Diego, Mid-City Normal Heights, Encanto, and North Park in the central part of San Diego, and the Mira Mesa Community planning area also had low heat mitigation index values for nighttime (Figures A10 and A11).

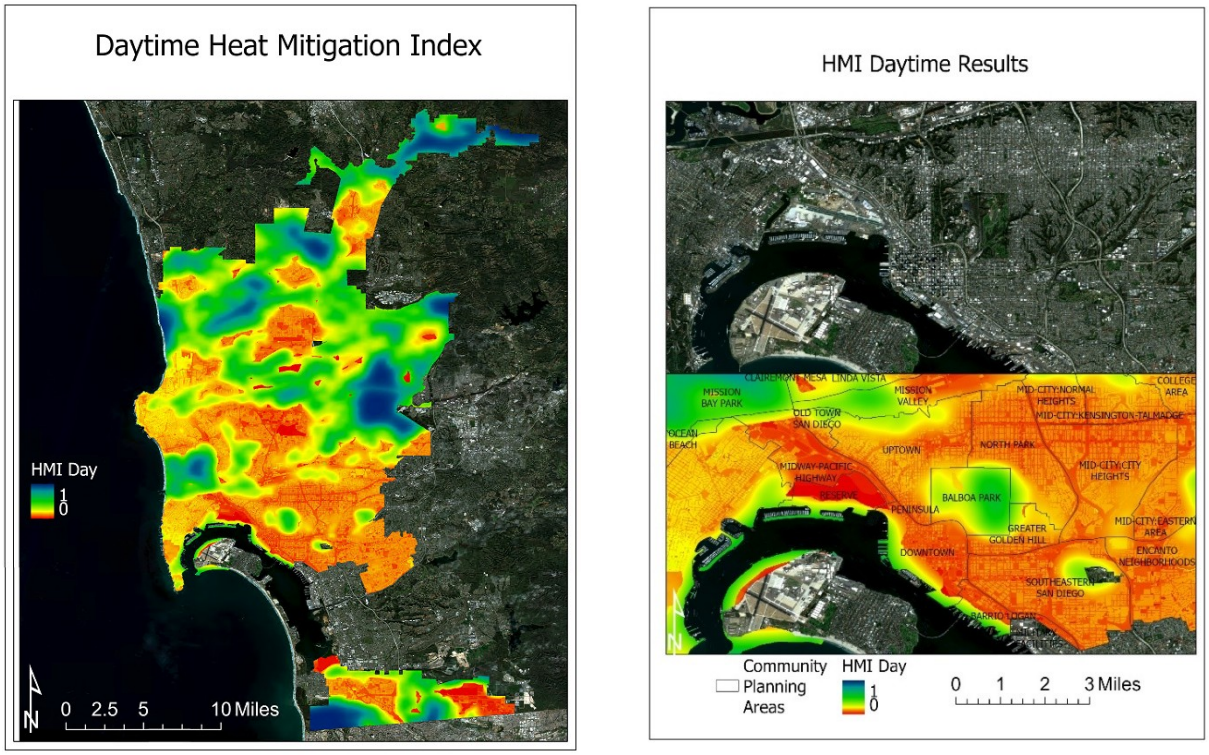

Figure 3: Daytime HMI (left) and Daytime HMI zoomed in on the San Diego Bay/downtown area (right) in San Diego for summer months (May 1 - September 30). Created with InVEST Urban Cooling Model

Additionally, there are differences in HMI between streets, freeways, residential neighborhoods, and commercial corridors (Figure 3). Roads tend to have a low cooling capacity since they have low shade, low albedo, and low ET. We can also see the difference between residential and commercial areas as commercial corridors tend to have a lower HMI.

Modeling the 5% tree canopy increase was completed by increasing the shade parameter for residential areas, road right of way, public spaces such as parks and schools, and minimally for commercial areas (Figure A13). This subsequently increased the HMI in these areas resulting in an overall temperature decrease of 0.35 degree Celsius or 0.6-degree Fahrenheit.

Evaluating the difference in daytime LST normalized and 1 – Day HMI provides a tool to understand if high temperatures occur where low HMI is modeled and vice versa. Red areas are where HMI underestimates cooling and blue areas are where it over estimates cooling (Figure A12). The ability for heat mitigation in areas along the coast and natural areas tend to be underestimated by the model. This enforces our observation that the InVEST model cannot capture the cooling effect of the ocean. Simultaneously this is a relatively narrow band along the coast approximately 400 m wide. The blue areas show where the modeled HMI overestimates cooling. This primarily occurs in developed areas. On average the HMI seems to overestimate cooling as the mean difference is negative.

4.2 Uncertainties/ Limitations

4.2.1 PCA Analysis
Our PCA for both census tract and census block group had a negative loading for our “Over 65” variable but a positive loading for out “Over 65 and Isolated” variable. Although it is expected that those who are living alone and over 65 would be more vulnerable, it would be expected that those who are over 65 would also be vulnerable. The “Over 65” variable possibly had a negative loading due to not having a variable in the PCA that could explain more of its variance, in this case a variable that looked at those who live alone. We do not expect this negative loading to be much of an issue since PC 4 only accounted for 10% and 14% of the variance in the census tract and census block group respectively. Furthermore, our scores for the vulnerability index gave equal weights to the variance in each principal component instead of assigning weights based on the variance. It could be that some social and health variables have a larger impact on vulnerability than others and so should be weighted more heavily when assessing vulnerability. Also, it is important to note that the lack of heat morbidity and mortality data prevented further investigation into the impacts of heat of populations throughout San Diego.

4.2.2 UHI identification
Work from others (Hajat et al., 2005; Schwartz et al., 2005; Zhang et al., 2012) explores the differences between day and nighttime temperatures in a UHI context. In this study we weighted nighttime temperatures twice as high as daytime, but this ratio could be tinkered with to get a better understanding of the temporal patterns associated with heat risk. Similarly, how one defines “night” may be important. Here, we used 11 PM to 4 AM as our night time span. However, the coolest times of day, and thus greatest indicator of urban heat are generally associated with dawn, which always happens after 4 AM regardless of season. This is important because the largest disparities between built and unbuilt areas may be associated with daytime, rather than nighttime temperatures. This becomes exacerbated when weighting occurs.

4.2.3 InVEST Urban Cooling Model
We used default values for parameters Green Area Maximum Cooling Distance (GAMCD) of 400 m and Air Temperature Maximum Blending Distance (ATMBD) of 500 m (McDonald et al., 2016; Zardo et al., 2017) an. The GAMCD determines the extent of the cooling effect of land uses labeled as green areas. This may change with climate, vegetation type, and air mixing dynamics.

The coastal location of San Diego introduced substantial error since InVEST is not equipped to account for the cooling effect of large bodies of water. Water has a very low cooling capacity according to the InVEST equations which does not reflect the moderating effect oceans have on the surrounding air temperature. In addition, evapotranspiration data is not available over water, which resulted in a cooling capacity of effectively zero for the ocean. Since some investigation has shown that ET over water is minimal, the impact on the overall results of the project is negligible. However, this lack of data amplified the error associated with the deficiency in the InVEST Model to account for the cooling effect of large water bodies.

We made decisions on how to relate the generalized building values to the land classifications, these were subjective decisions on what categories should fit where. In addition, the data used to determine the generalized building values were from Sacramento and used standard floor heights so the process of attaining the building intensity values came from allot of assumptions.

4.3 Future Work

Though we present a quantitative spatial analysis of urban heat hotspots and vulnerability in the City of San Diego, here we suggest several additional steps to expand the impact of our study. The InVEST model and vulnerability analyses can be applied across the San Diego metro or county-wide. The 2018 population of the City of San Diego was only ~43% of the total population of the county. The same heat exposure and vulnerability can be found in San Diego's suburbs, and heat exposure increases with distance from the ocean.

Our heat risk aims to predict which regions are more at risk to require hospital visits due to extreme heat. However, we did not have data on heat morbidity and mortality. Since we did not have data on our dependent variable, we used Principal Component Analysis on our social and health indicators, an unsupervised learning statistical method. Principal Component Analysis looks at variables that are correlation via an unobserved variable, in this case that unobserved variable is assumed to be heat morbidity and mortality. For future replications, it would be best to observe relationships of social, health, and environmental variables with heat morbidity and mortality, if that data is available.

InVEST inputs and default values have the opportunity to be refined and updated to better reflect the current conditions of the city. In addition, analyzing the intermediate outputs could provide insights into different components of the model. Lastly, model validation and statistical analysis is important to understanding how well the model is performing. Model validation could occur in a number of ways; there are scripts on GitHub provided by other users that could be utilized or the air temperature results could be compared to *in situ* air temperature measurements from weather stations. Additional work can be done to develop a method to estimate evapotranspiration over water.

5. Conclusions

This study demonstrates that the City of San Diego has substantially higher temperatures than areas of unbuilt landscape. The temperatures were seen to be cooler with closer proximity to the ocean. Nighttime LST was found to exhibit less of a gradient of temperatures further away from the ocean. In particular the community planning areas of Normal Heights, Eastern Area, and College Area experienced the warmest temperatures throughout the city. Areas that had lower heat risk tended to have lower amounts of impervious surfaces, less infrastructure, and higher tree canopy.

There were differences between areas of risk and heat exposure, meaning that higher heat areas do not necessarily correlate to higher vulnerability. Certain demographic groups including Latino and those without a high school diploma had higher exposure to both day and nighttime temperature. Our PCA allowed us to more closely examine the factors that put residents at risk. We found that in

particular health indicators including cardiovascular disease, obesity, and diabetes were the most important factor in explaining which residents are most at risk. At the block group level in the absence of available health data, percent Latino, percent high school diploma and English language proficiency were the most important factors.

We also provide insight into the distribution of heat mitigation throughout the urban landscape. By introducing these metrics, we were better able to quantify the impacts of major bodies of water and urban green areas greater than two hectares and increasing tree canopy scenario. This is important because it demonstrates not only how increasing tree canopy will reduce city temperatures, but also explores the role of water and open green spaces. Much of the work completed on InVEST highlights the limitations of the model and the need to develop the model and the inputs with a question or objective in mind so that the inputs can be tailored to the information that is being sought. The methods and workflow for the InVEST model may be used by future DEVELOP projects and the partners to better understand the cooling capacity of increased tree canopy. In addition, we discuss the errors and uncertainties which may help future teams develop their models and inputs. The InVEST model can be applied by our project partners to the greater San Diego metro area to get a better understanding of the cooling capacity of the landscape throughout the region.

6. Acknowledgments

A special thank you to Dr. Kenton Ross of the NASA Langley Research Center., and Dr. David Hondula, Associate Professor for the School of Geographical Sciences and Urban Planning at Arizona State University, Ryan Hammock, Fellow for the Arizona – Tempe NASA DEVELOP node, and to everyone at the City of San Diego for taking the time to collaborate with us. Additionally, we would like to thank Kristen O'Shea of the Thriving Earth Exchange for their help on the project. We are extremely grateful for the expertise, patience and guidance, and collaboration provided to us. Finally, we would like to acknowledge the help received from the Cincinnati Convington Urban Development Team at the Massachusetts DEVELOP Node.

7. Glossary

Albedo – the fraction of light that is reflected by a surface
Cooling Capacity (CC) – a measure of a system's ability to remove heat
Earth observations – Satellites and sensors that collect information about the Earth's physical, chemical, and biological systems over space and time
ECOsystem Spaceborne Thermal Radiometer Experiment on Space Station (ECOSTRESS) – satellite mission that aims to measure how the terrestrial biosphere changes in response to environmental changes such as water availability
Evapotranspiration – the sum of evaporation of water from land and other surfaces and through transpiration by plants
Heat Exposure— the magnitude of heat energy in a given area
Heat Mitigation Index (HMI)– an index to estimate temperature reduction by vegetation
Heat Risk— product of heat risk and vulnerability, takes into account temperature and pre-existing medical conditions and socioeconomic factors

Heat Vulnerability— a numerical value that takes into account temperature and pre-existing medical conditions and socioeconomic factors.
Integrated Valuation of Ecosystem Services and Tradeoffs (InVEST) – a suite of models used to map and value the goods and services from nature that benefit human life
Land Surface Temperature (LST) – the temperature of the surface of the Earth
Operational Land Imager (OLI) – sensor aboard the Landsat 8 satellite that measures visible, near-infrared, and shortwave infrared wavelengths
Thermal Infrared Sensor (TIRS) – sensor aboard the Landsat 8 satellite that measures both Earth's surface temperature and atmosphere temperature

8. References

Allen, Richard & Pereira, L. & Raes, D. & Smith, M. (1998). FAO Irrigation and drainage paper No. 56. Rome: Food and Agriculture Organization of the United Nations. 56. 26-40.

AppEEARS Team. (2020). Application for Extracting and Exploring Analysis Ready Samples (AppEEARS). Ver. 2.54.1. NASA EOSDIS Land Processes Distributed Active Archive Center (LP DAAC), USGS/Earth Resources Observation and Science (EROS) Center, Sioux Falls, South Dakota, USA. Accessed February 18, 2021. https://lpdaacsvc.cr.usgs.gov/appeears

Cooley, H., & Pacific Institute. (2012). *Social vulnerability to climate change in California*. Sacramento, CA: California Energy Commission.

Dialesandro, J., Brazil, N., Wheeler, S., & Abunnasr, Y. (2021). Dimensions of Thermal Inequity: Neighborhood Social Demographics and Urban Heat in the Southwestern US. *International Journal of Environmental Research and Public Health*, *18*(3), 941. https://doi.org/10.3390/ijerph18030941

Ferreira, L. S., & Duarte, D. H. S. (2019). Exploring the relationship between urban form, land surface temperature and vegetation indices in a subtropical megacity. *Urban Climate*, 27, 105-123. https://doi.org/10.1016/j.uclim.2018.11.002

Guirguis, K., (2018). Heat, disparities, and health outcomes in San Diego County's diverse climate zones. *GeoHealth*, *2(7)*, 212-223. https://doi.org/10.1029/2017GH000127

Hook, S., Hulley, G. (2019). *ECOSTRESS Cloud Mask Daily L2 Global 70 m V001*. NASA EOSDIS Land Processes DAAC. Accessed 2021-02-18 from https://doi.org/10.5067/ECOSTRESS/ECO2CLD.001. Accessed February 18, 2021.

Hook, S., Hulley, G. (2019). *ECOSTRESS Land Surface Temperature and Emissivity Daily L2 Global 70 m V001*. NASA EOSDIS Land Processes DAAC. Accessed 2021-02-18 from

https://doi.org/10.5067/ECOSTRESS/ECO2LSTE.001. Accessed February 18, 2021.

Hook, S., Fisher, J. (2019). *ECOSTRESS Evapotranspiration PT-JPL Daily L3 Global 70 m V001*. NASA EOSDIS Land Processes DAAC. Accessed 2021-02-18 from https://doi.org/10.5067/ECOSTRESS/ECO3ETPTJPL.001. Accessed February 18, 2021.

Krayenhoff, E. S., Moustaoui, M., Broadbent, A. M., Gupta, V., & Georgescu, M. (2018). Diurnal interaction between urban expansion, climate change and adaptation in US cities. *Nature Climate Change*, 8(12), 1097-1103. 10.1038/s41558-018-0320-9

McDonald, R., Kroeger, T., Boucher, T., Wang, L., & Salem, R. (2016). Planting healthy air: a global analysis of the role of urban trees in addressing particulate matter pollution and extreme heat. Planting healthy air: a global analysis of the role of urban trees in addressing particulate matter pollution and extreme heat. 10.1007/978-3-319-97013-4_8

Olmedo, G. F., Ortega-Farías, S., de la Fuente-Sáiz, D., Fonseca-Luego, D. & Fuentes-Peñailillo, F. (2016) Water: tools and function to estimate actual evapotranspiration using land surface energy balance models in R. *The R Journal*, 8:2, 352-369.

Shen, H., Huang, L., Zhang, L., Wu, P., & Zeng, C. (2016). Long-term and fine-scale satellite monitoring of the urban heat island effect by the fusion of multi-temporal and multi-sensor remote sensed data: A 26-year case study of the city of Wuhan in China. *Remote Sensing of Environment*, 172, 109-125. https://doi.org/10.3390/rs9060536

Taha, H. (2017). Characterization of urban heat and exacerbation: Development of a heat island index for California. *Climate,* 5(3), 59. https://doi.org/10.3390/cli5030059

Vahmani, P., Jones, A. D., & Patricola, C. M. (2019). Interacting implications of climate change, population dynamics, and urban heat mitigation for future exposure to heat extremes. *Environmental Research Letters*, 14(8), 084051. 10.1088/1748-9326/ab28b0

Wald, A. Emergency Department Visits and Costs for Heat-Related Illness Due to Extreme Heat or Heat Waves in the United States: An Integrated Review. *Nurs. Econ*. 2019, 37, 35.

Weinberger, K. R., Haykin, L., Eliot, M. N., Schwartz, J. D., Gasparrini, A., & Wellenius, G. A. (2017). Projected temperature-related deaths in ten large US metropolitan areas under different climate change scenarios. *Environment international*, 107, 196-204. doi: 10.1016/j.envint.2017.07.006

Zardo, L., Geneletti, D., Pérez-Soba, M., & Van Eupen, M. (2017). Estimating the cooling capacity of green infrastructures to support urban planning.

Ecosystem services, 26, 225-235. https://doi.or,
g/10.1016/j.ecoser.2017.06.016

9. Appendices

Appendix A

Table A1: Platforms and sensors used for analysis.

Platform & Sensor	Parameters	Use
Landsat 8 OLI/TIRS	Surface reflectance, Albedo, daytime LST	Between 2015-2020, the thermal band and surface reflectance were used to calculate the land surface temperature during daytime hours, albedo, and daytime LST were all inputs for the InVEST model.
ISS- ECOSTRESS	Evapotranspiration, Nighttime land surface temperature	Nighttime measurements of land surface temperature were gathered from ECOSTRESS to enhance the partners' understanding of urban heat dissipation and consequent neighborhood-level health concerns. Evapotranspiration rates were gathered from ECOSTRESS for use in the InVEST model.

Table A2: Summary of Inputs to InVEST Urban Cooling Model.

Input	Description	Source
Land Use/Land Cover	Code that defines the land use of that area, the municipal data used 100 different categories [raster]	City of San Diego (Online GIS Repository)
Biophysical Table	A table containing physical characteristics per land use code (and associated description) present in the LULC raster [csv]	Compiled by team
Shade	Derived from tree canopy, represents percent shaded area per land use [0-1]	City of San Diego (Online GIS Repository)
Albedo	Represents percent of energy reflected from surface per land use [0-1]	Landsat 8 OLI
Building Intensity	Represents the intensity of development, a normalized value of the ratio of floor area to land area per land use [0-1]	City of San Diego (Online GIS Repository) Generalized Building Values table (Sacramento Urban Development fall 2020, Appendix B)
Evapotranspiration	Normalized evapotranspiration values in mm [raster]	ISS ECOSTRESS ET
AOI	Vector polygon delineating area of interest and aggregation boundaries of census block groups	City of San Diego (Online GIS Repository)
Green Area Maximum Cooling Distance	Default used of 400m [m]	Model Documentation
Reference Air Temperature	Rural reference temperature, mean LST was used from chosen reference areas [degrees C]	Landsat 8 OLI

Magnitude of Urban Heat Island Affect	Magnitude of the UHI Effect: Difference between rural reference temperature and the maximum temperature observed in the city. (average was used since surface temperatures fluctuate more than air) [degrees C]	Landsat 8 OLI
Air Temperature Maximum Blending Distance	Air Temperature Maximum Blending Distance: Used default value 500 [m]	Model Documentation

Table A3: Overview of American Community Survey (ACS) sociodemographic data and Center for Disease Control (CDC) 500 cities health data used, area division, date, source, and retrieval method.

Dataset	Area Division	Date/Time	Source	Retrieval
Total Population B01001_001	Census tract	2018, 5-year estimate (2014-2018)	ACS	Tidycensus package in R
Ethnic Minority (Non-White) B03002_001	Census tract Census block group	2018, 5-year estimate (2014-2018)	ACS	Tidycensus package in R
Below Poverty Line B17021_002	Census tract	2018, 5-year estimate (2014-2018)	ACS	Tidycensus package in R
Without High School Diploma B15003_002-016	Census tract Census block group	2018, 5-year estimate (2014-2018)	ACS	Tidycensus package in R
65 Years and Older B01001_020-25 B01001_044-49	Census tract Census block group	2018, 5-year estimate (2014-2018)	ACS	Tidycensus package in R
65 Years and Older, Living Alone B09020_015 B09020_018	Census tract Census block group	2018, 5-year estimate (2014-2018)	ACS	Tidycensus package in R

Percent Latino	Census tract Census block group	2018, 5-year estimate (2014-2018)	ACS	Tidycensus package in R
Percent Asian	Census tract Census block group	2018, 5-year estimate (2014-2018)	ACS	Tidycensus package in R
Percent Black	Census tract Census block group	2018, 5-year estimate (2014-2018)	ACS	Tidycensus package in R
Household Language by Household Limited English-Speaking Status C16002:	Census tract Census block group	2018, 5-year estimate (2014-2018)	ACS	Tidycensus package in R
500 Cities: Census Tract-level Data (GIS Friendly Format)	2018 release Census Tract	2018	Center for Disease Control and Prevention (CDC)	CDC Website

Table A4: Heat Exposure Score table of top ten scoring census tracts (CTs).

	GEOID									
Variables		06073013103	06073002202	06073002302	06073002201	06073002707	06073001300	06073008349	06073002402	06073001600	06073002301
	Daytime LST (° F)	98.4	112.4	112.1	111.7	112.0	110.3	110.3	110.6	110.3	111.1
	Nighttime LST (° F)	74.3	59.7	59.8	60.0	59.5	60.4	60.2	59.8	59.8	59.1
	Heat Exposure Score	98.8	96.0	95.9	95.9	95.6	95.4	95.3	95.2	95.0	95.0

Table A5: Heat Vulnerability Score table of top ten scoring census tracts (CTs).

Variables	GEOID									
	06073010013	06073010005	06073002202	06073010103	06073005000	06073003101	06073003305	06073003502	06073004900	06073017014
Hypertension (%)	32	30.9	31.3	32.6	29.8	36.4	32.7	30.3	30	48.7
Pulmonary Disease (%)	7.5	6.7	7.6	7	7.3	6.2	6.9	7.1	6.8	7.9
Heart Disease (%)	7.7	7.1	7	7.4	6.6	6.5	5.9	6.1	6.4	12.3
Asthma (%)	9.7	9.2	9.5	8.8	9.7	9.8	10.6	10.3	9.8	7.2
Diabetes (%)	16.7	15.6	15.4	14.7	14.7	14.5	14.4	14.3	14.3	14.1
Obesity (%)	31.5	28.6	27.6	28.4	32.1	28.5	30.6	31.4	31.1	15.8
No Health Insurance (%)	16.6	14.0	23.3	9.15	24.2	18.2	12.5	20.0	19.2	1.83
Poverty (%)	29.2	28.6	39.6	18.0	37.7	20.0	36.5	36.7	27.3	5.15
No HS Diploma (%)	53.5	38.7	46.6	33.5	43.4	19.2	37.5	39.1	45.0	4.16
Limited English Proficiency (%)	28.8	27.8	31.9	16.0	33.8	4.42	18.6	16.9	17.7	2.39
Latinx Population (%)	97.1	93.6	72.3	71.1	85.3	59.5	60.1	80.8	85.9	6.87
Black Population (%)	0.9	0.5	5.4	4.9	4.9	32.2	25.8	10.1	3.4	1.4
Asian Population (%)	0.1	2.9	12.5	3.38	0.9	2.7	7.45	2.0	1.3	6.0
Non-White (%)	11.9	14.8	43.7	27.7	34.3	64.7	58.5	50.4	35.4	11.0
Over 65 (%)	18.5	21.7	18.8	13.8	14.2	16.1	18.7	13.6	12.3	75.3
Over 65 and Alone (%)	1.4	3.7	17.0	1.7	11.9	4.1	9.3	0	12.3	8.2
Heat Vulnerability Score	9.3	8.2	8.0	7.3	7.3	7.3	7.0	6.9	6.9	6.7

Table A6: Heat Risk Score table of top ten scoring census tracts (CTs).

Variables	GEOID									
	06073002202	06073013103	06073002302	06073002707	06073017014	06073010013	06073002201	06073002402	06073003101	06073002712
Hypertension (%)	31.3	28.1	29.2	28.1	48.7	32	27.4	26.4	36.4	31.9
Pulmonary Disease (%)	7.6	5.7	7	6.6	7.9	7.5	6.2	6.1	6.2	6.5
Heart Disease (%)	7	5.6	5.8	5.1	12.3	7.7	4.6	4.8	6.5	6.4
Asthma (%)	9.5	9	9.9	10	7.2	9.7	10.1	9.8	9.8	9.6
Diabetes (%)	15.4	11.8	13.9	12.8	14.1	16.7	11.4	11.8	14.5	13
Obesity (%)	27.6	26.1	27.2	28	15.8	31.5	29	28.1	28.5	25.7
No Health Insurance (%)	23.3	10.4	21.0	22.1	1.8	16.6	16.8	24.2	18.2	5.5
Poverty (%)	39.6	14.2	31.3	33.2	5.1	29.2	42.1	29.7	20.0	26.2
No HS Diploma (%)	46.6	35.0	49.9	41.9	4.2	53.5	42.7	46.9	19.2	22.6
Limited English Proficiency (%)	31.9	17.5	28.9	22.5	2.4	28.8	25.3	22.9	4.4	17.6
Latinx Population (%)	72.3	75.8	63.2	58.3	6.9	97.1	47.2	68.5	59.5	38.1
Black Population (%)	5.4	3.0	4.1	9.9	1.4	0.9	22.7	14.3	32.2	25.8
Asian Population (%)	12.5	5.1	23.0	21.4	6.0	0.1	20.5	12.8	2.7	16.2
Non-White (%)	43.7	26.8	51.7	51.8	11.0	11.9	55.1	44.6	64.7	62.6
Over 65 (%)	18.8	17.3	10.2	9.2	75.3	18.5	6.9	10.6	16.1	22.0
Over 65 and Alone (%)	17.0	0	14.8	10.1	8.2	1.4	16.8	9.0	4.1	8.7
Daytime LST (° F)	112.4	98.4	112.1	112.0	108.1	105.1	111.7	110.6	105.1	106.4
Nighttime LST _(° F)	59.7	74.3	59.8	59.5	60.4	59.0	60.0	59.8	60.2	60.4
Heat Risk Index	0.76	0.71	0.68	0.61	0.61	0.57	0.56	0.55	0.53	0.52

Table A7: Difference to the mean table of top ten scoring census tracts' social and health indicators (CTs).

	GEOID									
Variables	06073002202	06073013103	06073002302	06073002707	06073017014	06073010013	06073002201	06073002402	06073003101	06073002712
Hypertension (%)	9.5	6.3	7.4	6.3	26.9	10.2	5.6	4.6	14.6	10.1
Pulmonary Disease (%)	3.7	1.8	3.1	2.7	4.0	3.56	2.3	2.2	2.3	2.6
Heart Disease (%)	3.0	1.6	1.8	1.1	8.3	3.7	0.6	0.8	2.5	2.4
Asthma (%)	2.3	1.8	2.7	2.8	0.04	2.5	2.9	2.6	2.6	2.4
Diabetes (%)	8.0	4.4	6.5	5.4	6.7	9.3	4.0	4.4	7.1	5.6
Obesity (%)	9.7	8.2	9.3	10.1	-2.1	13.6	11.1	10.2	10.6	7.8
No Health Insurance (%)	14.7	1.8	12.3	13.5	-6.8	8.0	8.2	15.7	9.7	-3.1
Poverty (%)	26.3	0.9	18.0	19.9	-8.2	15.9	28.8	16.4	6.7	12.9
No HS Diploma (%)	34.0	22.4	37.3	29.3	-8.4	40.9	30.1	34.3	6.6	10.0
Limited English Proficiency (%)	24.5	10.1	21.5	15.1	-5.0	21.5	18.0	15.5	-2.9	10.2
Latinx Population (%)	41.	45.0	32.4	27.	-23.9	66.3	16.39	37.6	28.6	7.3
Black Population (%)	-0.5	-2.9	-1.8	3.9	-4.6	-5.0	16.7	8.4	26.3	19.9
Asian Population (%)	-1.5	-8.9	8.9	7.3	-8.0	-13.9	6.5	-1.2	-11.3	2.2

	Non-White (%)	11.6	-5.8	19.2	19.3	-21.5	-20.6	22.5	12.6	32.1	30.0
	Over 65 (%)	0.3	-1.2	-8.3	-9.2	56.8	0.03	-11.5	-7.8	-2.3	3.5
	Over 65 and Alone (%)	7.5	-9.5	5.3	0.6	-1.3	-8.1	7.3	-0.5	-5.4	-0.8

Table A8: Heat Exposure Score table of top ten scoring census block groups (CBGs).

	GEOID									
Variables		060730131031	060730022021	060730013002	060730027074	060730022012	060730023023	060730022022	060730017001	060730013005	060730093011
	Daytime LST	98.4	114.8	112.6	113.3	112.5	112.9	113.2	110.4	110.5	109.8
	Nighttime LST	74.3	60.0	60.4	60.0	60.2	60.0	59.7	61.1	61.0	61.2
	Exposure Score	82.4	78.0	77.8	77.8	77.6	77.6	77.6	77.5	77.5	77.4

Table A9: Heat Vulnerability Score table of top ten scoring census block groups (CBGs).

	GEOID									
Variables	060730009003	060730027091	060730027123	060730022011	060730009005	060730025013	060730009006	060730030011	060730033051	060730027083
No HS Diploma (%)	2.0	58.2	33.0	35.4	0	30.7	12.7	1.9	25.1	45.3
Limited English Proficiency (%)	11	26	27	32	13	28	5	14	23	31
Latinx Population (%)	23.6	57.5	46.1	28.8	15.1	53.9	38.8	17.7	30.4	42.0
Black Population (%)	28	30	39	33	24	17	14	57	41	30
Asian Population (%)	10.2	9.0	3.2	31.0	4.9	16.2	3.3	12.6	21.3	20.4
Non-White (%)	50.6	49.4	67.6	77.6	36.3	51.3	43.4	85.8	69.0	63.0
Over 65 (%)	1.7	2.7	6.9	9.9	2.4	3.2	3.2	26.3	16.9	9.4
Over 65 and Alone (%)	100	37	21	8	100	41	100	7	8	0
Heat Vulnerability Score	6.3	6.1	5.9	5.8	5.4	5.0	4.9	4.9	4.9	4.9

Table A10: Heat Risk Score table of top ten scoring census block groups (CBGs).

	GEOID									
Variables	060730022011	060730009003	060730131031	060730022012	060730027083	060730018003	060730009005	060730024021	060730009006	060730027123
No HS Diploma (%)	35.4	2.0	46.5	51.3	45.3	17.3	0	43.2	12.7	33.0
Limited English Proficiency (%)	32	11	24	18	31	0	13	20	5	27
Latinx Population (%)	28.8	23.6	92.2	67.8	42.0	10.6	15.1	67.7	38.8	46.1
Black Population (%)	33	28	0	11	30	40	24	20	14	39
Asian Population (%)	31.0	10.2	0.5	8.9	20.4	28.6	4.9	8.6	3.3	3.2
Non-White (%)	77.6	50.6	16.2	29.9	62.9	77.6	36.3	42.0	43.4	67.6
Over 65 (%)	9.9	1.7	15.0	3.4	9.4	7.3	2.4	6.0	3.2	6.9
Over 65 and Alone (%)	8	100	0	48	0	0	100	30	100	21
Daytime LST (° F)	111.3	108.8	98.4	112.5	112.9	110.2	108.0	112.3	108.7	106.3
Nighttime LST (° F)	60.0	60.6	74.3	60.2	58.8	60.7	60.6	59.6	60.6	60.8
Heat Risk Index	0.6	0.	0.6	0.6	0.6	0.6	0.5	0.5	0.5	0.

Table A11: InVEST biophysical table current conditions input.

lucode	lulc_desc	shade	kc	albedo	green_area	building_intensity
0	No data	0	0	0	0	0
1000	Spaced Rural Residential	0.20	1	0.15	0	0.04
1090	Spaced Rural Residential Without Units	0.55	1	0.13	0	0.06
1110	Single Family Detached	0.18	1	0.15	0	0.25
1120	Single Family Multiple-Units	0.18	1	0.15	0	0.28
1190	Single Family Residential Without Units	0.27	1	0.15	0	0.09
1200	Multi-Family Residential	0.19	1	0.14	0	0.81
1280	Single Room Occupancy Units (SRO's)	0.10	1	0.19	0	0.36
1290	Multi-Family Residential Without Units	0.17	1	0.14	0	0.62
1300	Mobile Home Park	0.095	1	0.19	0	0.85
1401	Jail/Prison	0.0070	1	0.23	0	0.61
1402	Dormitory	0.20	1	0.14	0	0.40
1403	Military Barracks	0.093	1	0.18	0	0.40
1404	Monastery	0.35	1	0.15	0	0.39
1409	Other Group Quarters	0.18	1	0.15	0	0.69

	Facility					
1501	Hotel/Motel (Low-Rise)	0.19	1	0.14	0	0.62
1502	Hotel/Motel (High-Rise)	0.16	1	0.15	0	1.00
1503	Resort	0.28	1	0.13	0	0.42
2001	Heavy Industry	0.018	1	0.14	0	0.28
2101	Industrial Park	0.14	1	0.16	0	0.24
2103	Light Industry - General	0.10	1	0.17	0	0.24
2104	Warehousing	0.07	1	0.18	0	0.26
2105	Public Storage	0.081	1	0.18	0	0.30
2201	Extractive Industry	0.047	1	0.18	0	0.0021
2301	Junkyard/Dump/Landfill	0.0096	1	0.16	0	0.0057
4101	Commercial Airport	0.0066	1	0.18	0	0.065
4102	Military Airport	0.0019	1	0.2	0	0.026
4103	General Aviation Airport	0.0053	1	0.17	0	0.028
4104	Airstrip	0.0053	1	0.17	0	0.028
4111	Rail Station/Transit Center	0.11	1	0.15	0	0.066
4112	Freeway	0.083	1	0.15	0	0.00081
4113	Communications and Utilities	0.081	1	0.15	0	0.044
4114	Parking Lot - Surface	0.093	1	0.14	0	0.033
4115	Parking Lot - Structure	0.10	1	0.178	0	0.50
4116	Park and Ride Lot	0.12	1	0.15	0	0.079
4117	Railroad Right of Way	0.077	1	0.14	0	0.0064
4118	Road Right of Way	0.11	1	0.15	0	0.0041
4119	Other Transportation	0.035	1	0.18	0	0.10
4120	Marine Terminal	0.00061	1	0.15	0	0.22
5001	Wholesale Trade	0.077	1	0.17	0	0.66
5002	Regional Shopping Center	0.10	1	0.18	0	0.78

5003	Community Shopping Center	0.083	1	0.14	0	0.61
5004	Neighborhood Shopping Center	0.098	1	0.13	0	0.60
5005	Specialty Commercial	0.19	1	0.14	0	0.59
5006	Automobile Dealership	0.041	1	0.15	0	0.50
5007	Arterial Commercial	0.065	1	0.15	0	0.91
5008	Service Station	0.095	1	0.14	0	0.12
5009	Other Retail Trade and Strip Commercial	0.074	1	0.16	0	0.17
6001	Office (High-Rise)	0.14	1	0.16	0	0.42
6002	Office (Low-Rise)	0.18	1	0.14	0	0.21
6003	Government Office/Civic Center	0.12	1	0.16	0	0.33
6101	Cemetery	0.22	1	0.17	1	0.035
6102	Religious Facility	0.15	1	0.15	0	0.31
6103	Library	0.21	1	0.14	0	0.30
6104	Post Office	0.069	1	0.16	0	0.36
6105	Fire/Police Station	0.14	1	0.15	0	0.24
6108	Mission	0.47	1	0.13	0	0.17
6109	Other Public Services	0.18	1	0.16	0	0.26
6501	UCSD/VA Hospital/Balboa Hospital	0.17	1	0.17	0	0.43
6502	Hospital - General	0.12	1	0.16	0	0.45
6509	Other Health Care	0.14	1	0.15	0	0.39
6701	Military Use	0.057	1	0.15	0	0.066
6702	Military Training	0.0039	1	0.12	0	0.0034
6703	Weapons Facility	0.011	1	0.14	0	0.014
6801	SDSU/CSU San Marcos/UCSD	0.24	1	0.15	0	0.28
6802	Other University or College	0.19	1	0.14	0	0.24
6803	Junior College	0.11	1	0.17	0	0.28
6804	Senior High School	0.092	1	0.17	0	0.11
6805	Junior High School or Middle School	0.073	1	0.17	0	0.11

6806	Elementary School	0.096	1	0.15	0	0.12
6807	School District Office	0.12	1	0.16	0	0.20
6809	Other School	0.15	1	0.15	0	0.14
7201	Tourist Attraction	0.19	1	0.15	0	0.037
7202	Stadium/Arena	0.031	1	0.14	0	0.084
7203	Racetrack	0.031	1	0.14	0	0.084
7204	Golf Course	0.16	1	0.19	1	0.0018
7205	Golf Course Clubhouse	0.19	1	0.15	0	0.070
7206	Convention Center	0.081	1	0.17	0	0.70
7207	Marina	0.045	1	0.15	0	0.016
7208	Olympic Training Center	0.19	1	0.15	0	0.037
7209	Casino	0.19	1	0.14	0	0.59
7210	Other Recreation - High	0.13	1	0.16	0	0.055
7211	Other Recreation - Low	0.027	1	0.12	0	0.0035
7601	Park - Active	0.16	1	0.17	1	0.011
7603	Open Space Park or Preserve	0.11	1	0.17	1	0.00038
7604	Beach - Active	0.042	1	0.22	0	0.0033
7605	Beach - Passive	0.0078	1	0.15	0	0.00074
7606	Landscape Open Space	0.27	1	0.14	1	0.0085
7607	Residential Recreation	0.28	1	0.15	0	0.036
7609	Undevelopable Natural Area	0.15	1	0.13	1	0.000033
8001	Orchard or Vineyard	0.29	1	0.15	1	0.0012
8002	Intensive Agriculture	0.08	1	0.18	1	0.014
8003	Field Crops	0.087	1	0.16	1	0.0035
9101	Vacant and Undeveloped Land	0.038	1	0.13	0	0.0040
9200	Water	0	1	0.17	1	0
9201	Bay or Lagoon	0.00032	1	0.098	1	0.00066
9202	Lake/Reservoir/Large Pond	0.067	1	0.13	0	0.00029
9501	Residential Under Construction	0.060	1	0.20	0	0.049

9502	Commercial Under Construction	0.047	1	0.17	0	0.24
9503	Industrial Under Construction	0.027	1	0.19	0	0.050
9504	Office Under Construction	0.125789	1	0.16	0	0.15
9505	School Under Construction	0.21	1	0.21	0	0.0013
9506	Road Under Construction	0.050	1	0.15	0	0.032
9507	Freeway Under Construction	0.083	1	0.15	0	0.00081
9700	Mixed Use	0.045	1	0.17	0	0.34

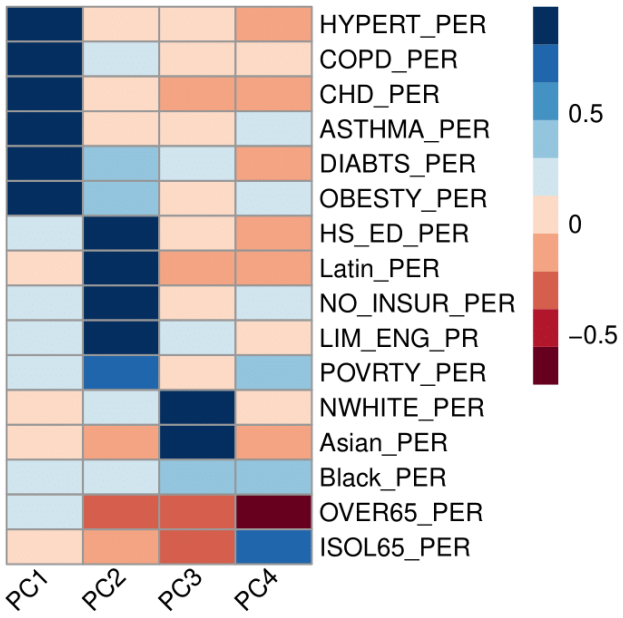

Figure A1: Principal component analysis correlation map of social and health indicators.

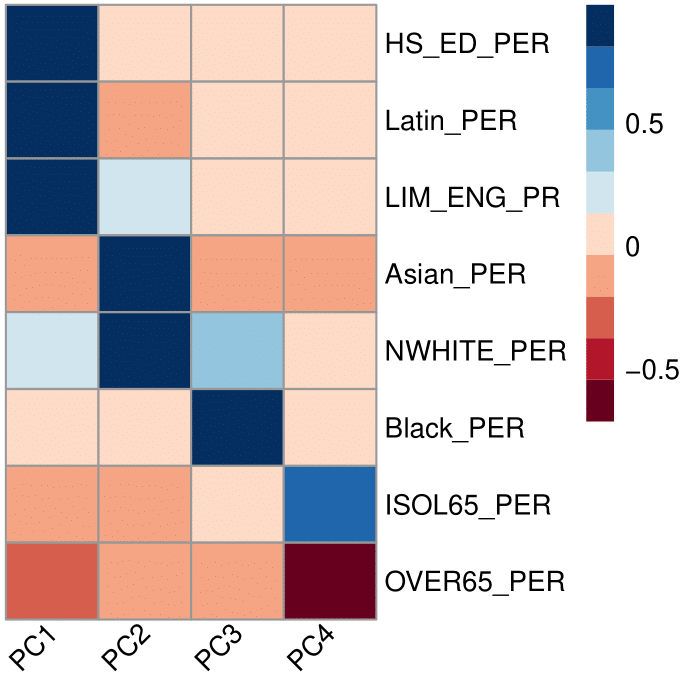

Figure A2: Principal component analysis for social indicators for census block groups.

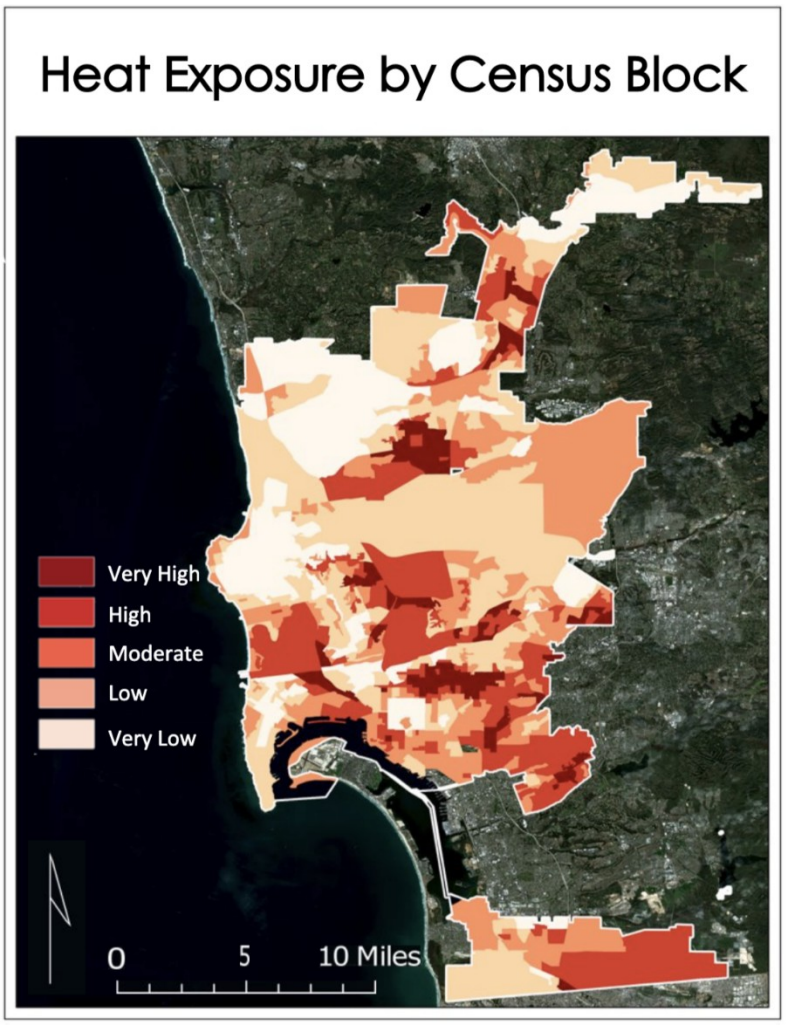

Figure A3: Heat exposure by census block group. Created with 2016-2020 average daytime urban heat island (UHI) magnitude (Landsat 8 imagery) and average night-time urban heat island magnitude (ECOSTRESS imagery) in the City of San Diego.

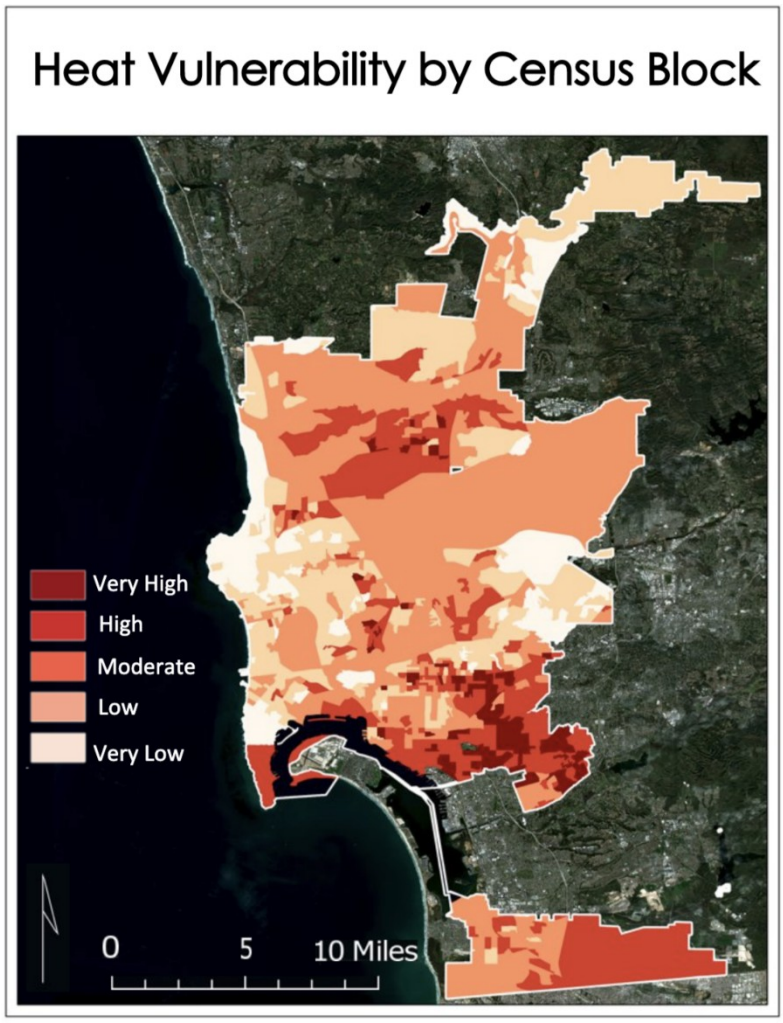

Figure A4: Heat vulnerability by census block group. Note that this was computed using social variables only.

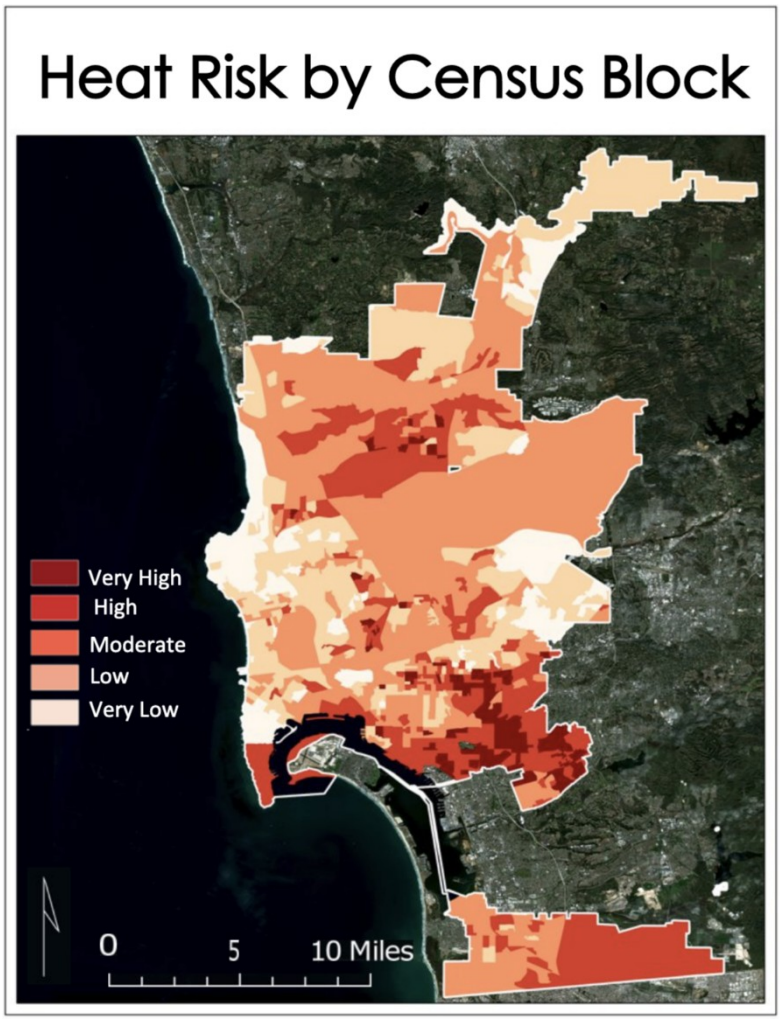

Figure A5: Heat risk by census block group. Note that the vulnerability index was computed using social variables.

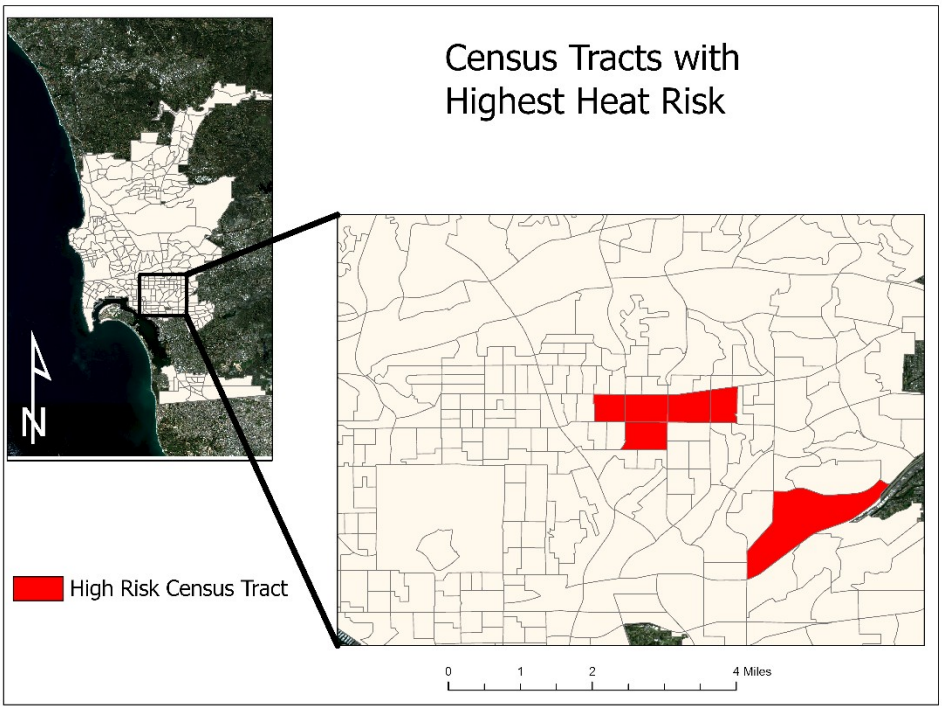

Figure A6: Map of highest risk census tracts.

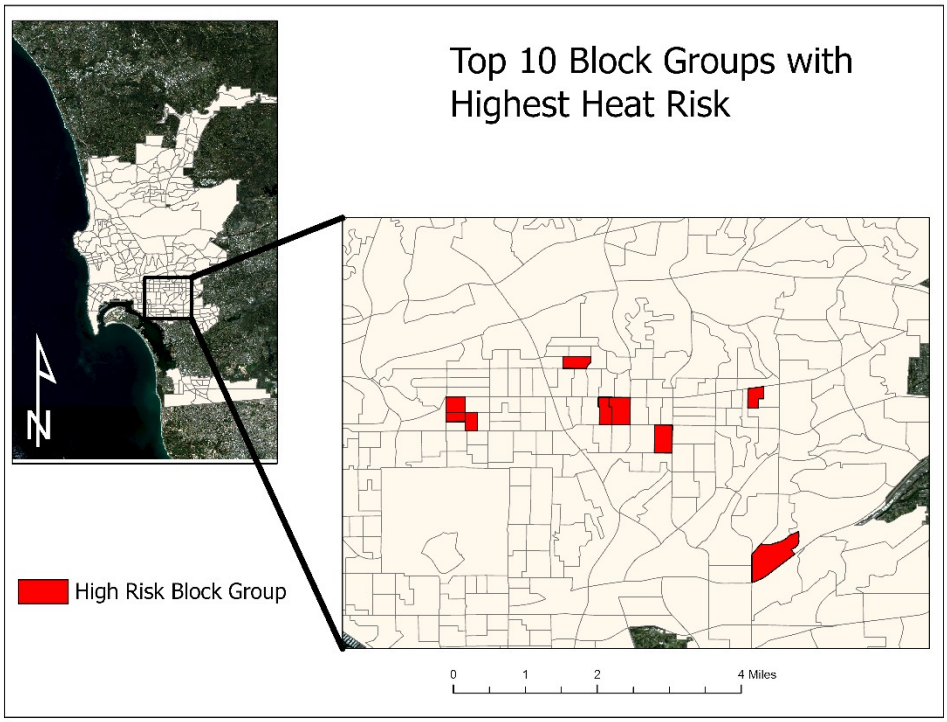

Figure A7: Map of top 10 highest risk block groups.

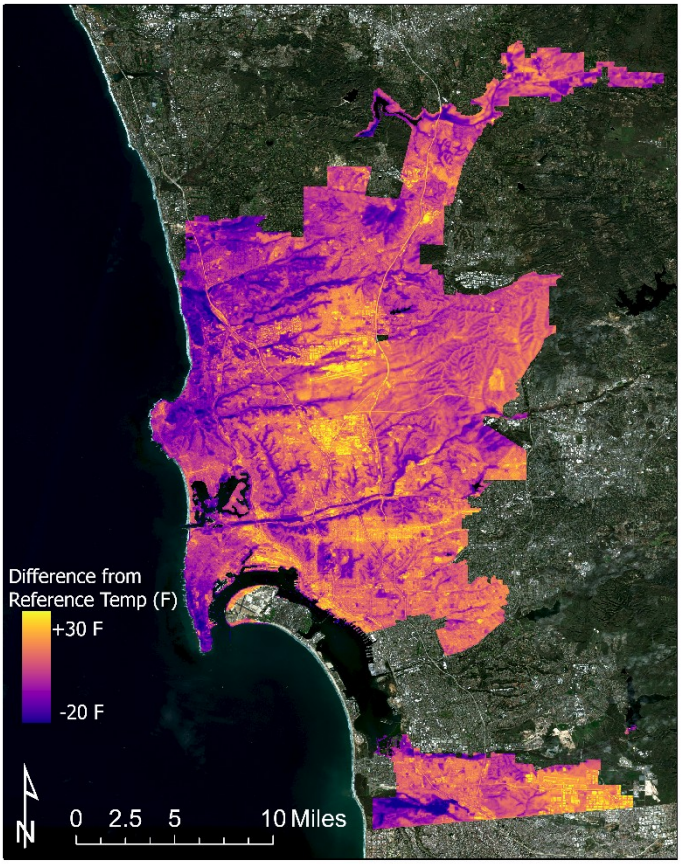

Figure A8: Daytime temperature departure from reference site LST (F°). Created with 2016-2020 average daytime urban heat island (UHI) magnitude (Landsat 8 imagery).

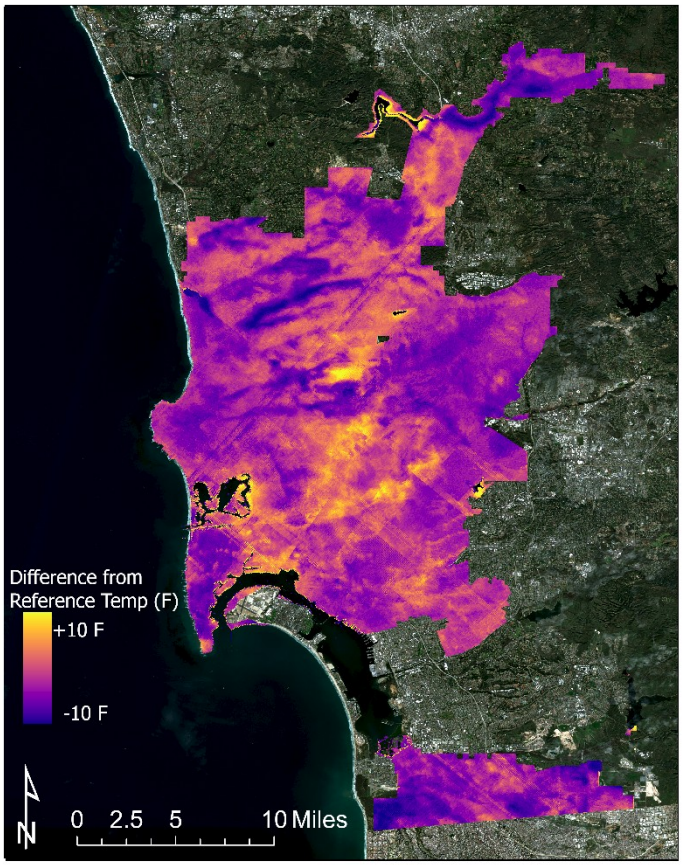

Figure A9: Nighttime temperature departure from reference site LST (F°). Created with 2018-2020 average night-time urban heat island magnitude (ECOSTRESS imagery) in the City of San Diego.

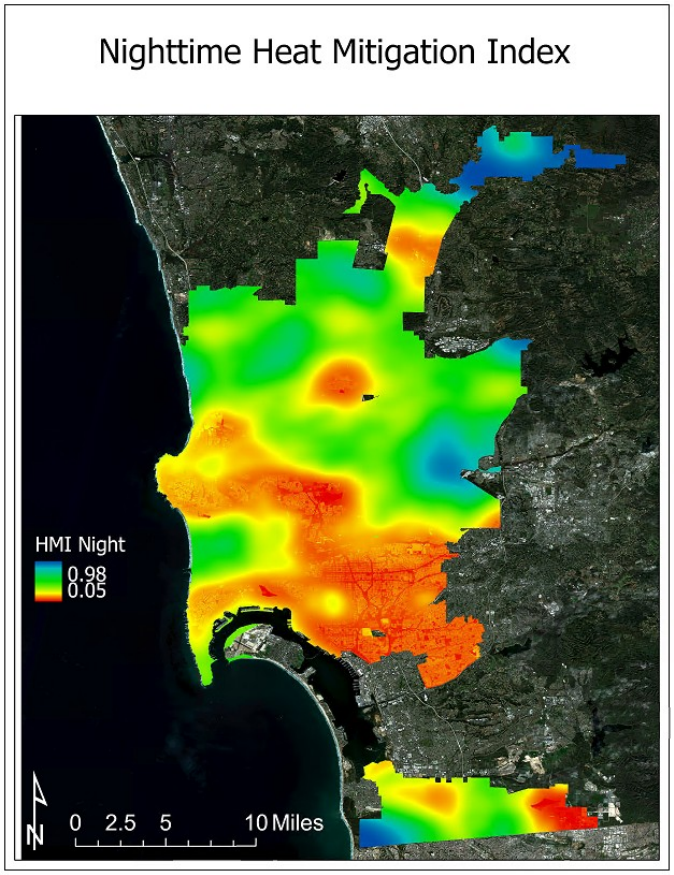

Figure A10: Nighttime Heat Mitigation Index San Diego Bay/Downtown Area for summer months (May 1 – September 30) nighttime cooling capacity in San Diego, CA, 2021 (created with InVEST Urban Cooling Model).

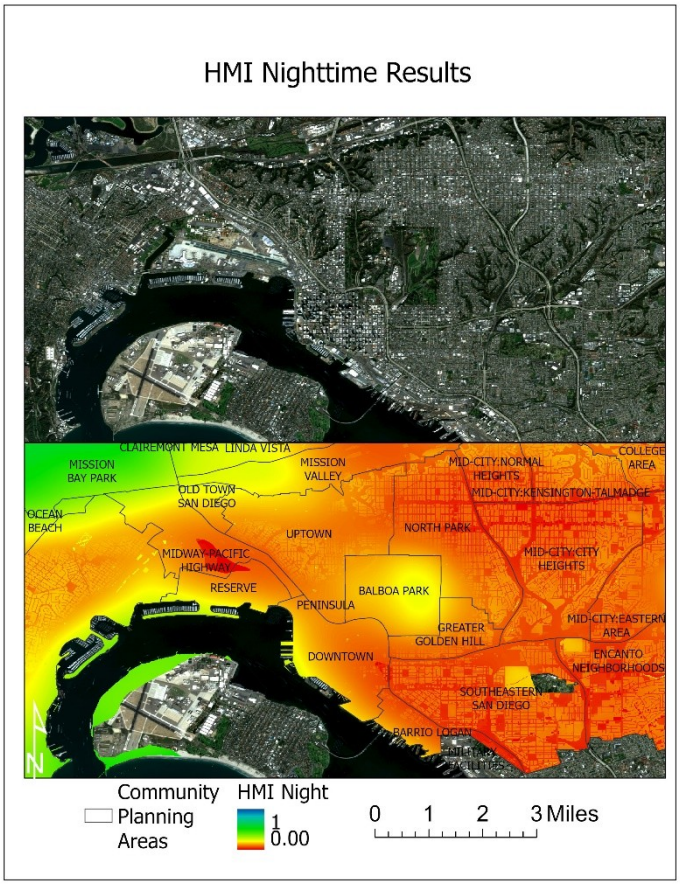

Figure A11: Nighttime Heat Mitigation Index Zoomed in on San Diego Bay/Downtown Area for summer months (May 1 – September 30) nighttime cooling capacity in San Diego, CA, 2021 (created with InVEST Urban Cooling Model).

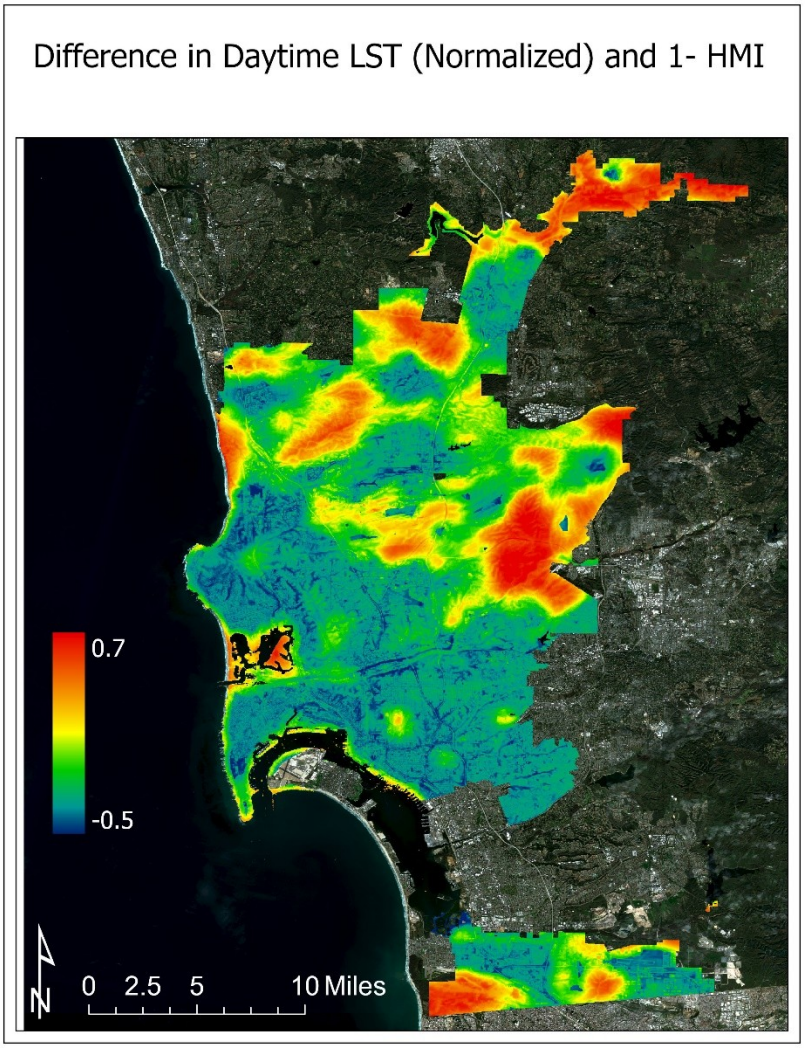

Figure A12: Difference in Daytime LST (Normalized) and 1 – Daytime Heat Mitigation Index daytime cooling capacity in San Diego, CA, 2021 (created with InVEST Urban Cooling Model).

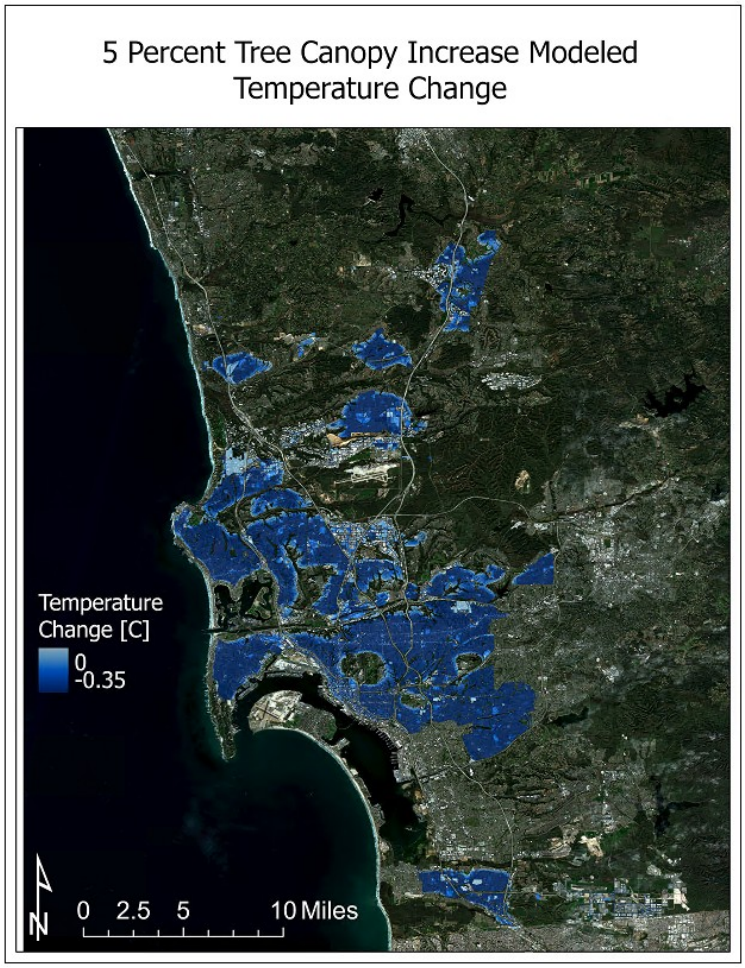

Figure A13: Change in temperature due to modeled 5% overall increase in tree canopy.